

Solution of Maxwell's Equation

A Numerical Approximation

by

ABDENNASER HADAB

Under the supervision of

PROF. DR.-ING. L. BERGER

M. SC. S. SCHOLZ

بِسْمِ اللَّهِ الرَّحْمَنِ الرَّحِيمِ

A written report of the Bachelor thesis

Solution of Maxwell's Equation: A Numerical Approach

Abdennaser Hadab

Under the supervision of:
Prof. Dr.-Ing. L. Berger
M. Sc. S. Scholz

September 1, 2023

Hochschule Ravensburg-Weingarten University of Applied
Sciences



Disclaimer

I hereby declare that this dissertation is my own original work and has not been submitted before to any institution for assessment purposes.

Colophon

This document was typeset with the help of *KOMA-Script* and \LaTeX using the *kaobook* class.

The source code of this book is available at:

<https://github.com/fmarotta/kaobook>

Contents

Contents	vi
1 Context and Overview	1
1.1 Context And Overview	1
1.1.1 Introduction	1
1.1.2 Background	1
1.1.3 Objectives	1
1.1.4 Thesis Outline	2
PART 1: THEORETICAL APPROACH	3
2 A Contextual Introduction to Maxwell's Equations	4
2.1 Historical context of Maxwell's equations	4
2.2 Overview of Maxwell's equations	6
2.2.1 Faraday's law	6
2.2.2 Gauss's law	6
2.3 Applications	7
3 Maxwell's Equations: The Math	8
3.1 First the basics!	8
3.1.1 A little bit of math	8
3.1.2 Coulomb's law	11
3.1.3 Electric field	12
3.1.4 Lorentz Force	13
3.1.5 Magnetic Field	13
3.1.6 Principle of charge conservation	14
3.2 The four equations	15
3.2.1 Local form	15
3.2.2 Integral form	16
4 A Numerical Approximation	19
4.1 Defining the framework	19
4.1.1 So what is the FTDT?	19
4.1.2 The Yee Grid	19
4.2 Discretizing the equations	23
4.2.1 Maxwell-Faraday	23
4.2.2 Maxwell-Ampère	29

4.2.3	Maxwell-Flux	31
4.2.4	Maxwell-Gauss	31
4.2.5	Final discretized grid equation	31
5	Creation and Testing of a Simplified FDTD Algorithm	33
5.1	The code	33
5.2	Result of the Simulation	37
	APPENDIX	39

List of Figures

2.1 Michael Faraday	4
2.2 James Clerk Maxwell	5
2.3 Faraday's induction experiment	6
2.4 The BAA	7
3.1 Stokes' theorem	10
3.2 Ostrogradsky's theorem	11
3.3 Coulomb's force of charge q_1 on charge q_2	11
3.4 Electric field of Q with q as test charge	12
3.5 Lorentz Force	13
3.6 A surface current distribution	14
4.1 A surface current distribution	19
4.2 3D Yee Grid	20
4.3 A co-located grid	22
4.4 A staggered grid	22
4.5 Comparison between staggered and co-located grid	23
4.6 Elementary cell integration scheme	24
4.7 Elementary cell integration surface	24
4.8 The dual grid \tilde{G}	29
4.9 Conversion between analog and discretized M-Es	32
5.1 The simulation result	37

List of Tables

2.1 Key historical events leading to the establishment of Maxwell's equations . .	5
---	---



1 Context and Overview

1.1 Context And Overview

1.1.1 Introduction

In this chapter, we provide an overview of the context and background of this bachelor thesis. We discuss the motivation behind our research and the importance of Maxwell's equations in the field of electromagnetism.

1.1.2 Background

Electromagnetism is a fundamental branch of physics that deals with the interactions between electrically charged particles. Maxwell's equations, named after the Scottish physicist James Clerk Maxwell, are a set of four equations that describe the behavior of electric and magnetic fields and their relationship to charges and currents.

1.1.3 Objectives

The objective of this thesis is to provide a comprehensive understanding of Maxwell's equations and their numerical approximation using the finite-difference time-domain (FDTD)¹ method. Specifically, we aim to:

- ▶ Explain the theory behind Maxwell's equations and their applications
- ▶ Describe the FDTD method and its implementation for solving Maxwell's equations numerically
- ▶ Present and discuss the results of simulations that we have performed using the FDTD method

1.1 Context And Overview	1
1.1.1 Introduction	1
1.1.2 Background	1
1.1.3 Objectives	1
1.1.4 Thesis Outline	2

¹: Will be abbreviated as so for the rest of this dissertation.

1.1.4 Thesis Outline

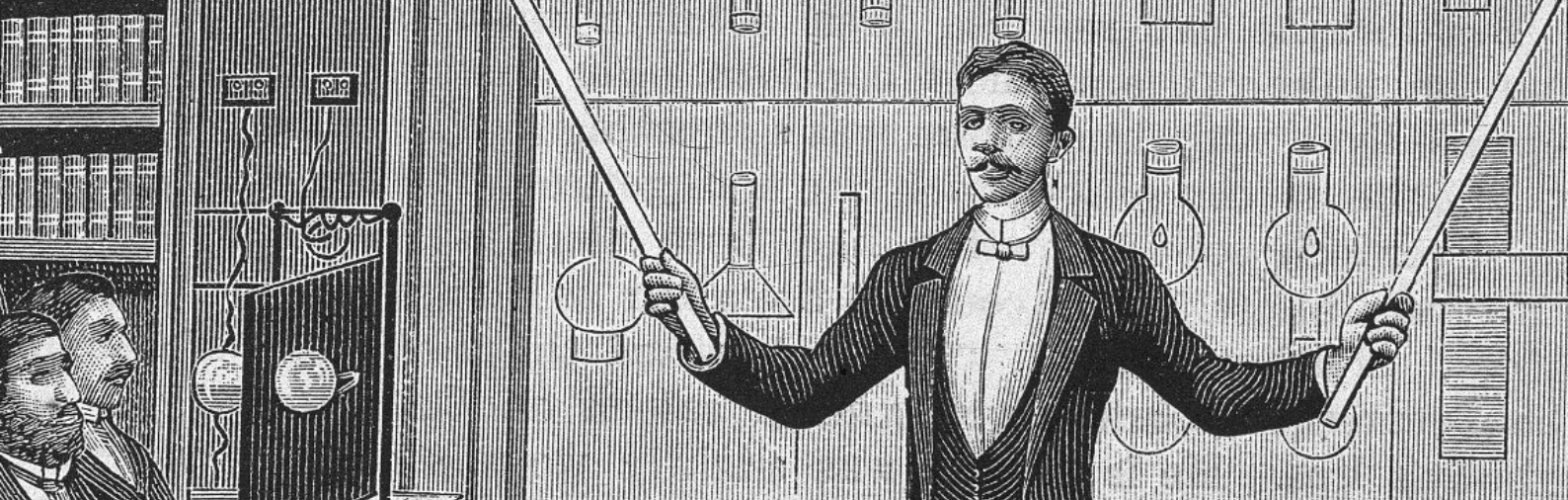
This thesis is structured as follows:

1. Chapter 1: Context and Overview (this chapter)
2. Chapter 2: Maxwell's Equations: The History
3. Chapter 3: Maxwell's Equations: The Math
4. Chapter 4: Introduction to FDTD
5. Chapter 5: Simulation and results

In Chapter 2, we provide a detailed explanation of Maxwell's equations, including their historical context, applications, and significance. In Chapter 3, we lay down the mathematical foundation behind the equations. Following in chapter 4, we describe the FDTD method and its application to Maxwell's equations. Chapter 5 contains the results of simulations that we have performed using the FDTD method.

Overall, this thesis aims to provide a comprehensive understanding of Maxwell's equations and their numerical approximation using the FDTD method, as well as their applications and historical context.

PART 1: THEORETICAL APPROACH



2 A Contextual Introduction to Maxwell's Equations

2.1 Historical context of Maxwell's equations

The history of electromagnetism can be traced back to the 18th century, when scientists first began studying the behavior of electric charges. In 1785, Charles-Augustin de Coulomb formulated Coulomb's law, which described the force between two electric charges. This work laid the foundation for further research into the nature of electricity and magnetism.

In the early 19th century, Carl Friedrich Gauss built upon Coulomb's work and developed the theory of the magnetic potential. He introduced the concept of magnetic flux, which described the flow of magnetic lines of force through a closed surface. Gauss's work paved the way for further research into the relationship between electric and magnetic fields.

Michael Faraday's experiments in the mid-19th century showed that an electric current could produce a magnetic field and that a changing magnetic field could produce an electric current. He also introduced the concept of lines of force, which he used to describe the behavior of electric and magnetic fields. Faraday's work established the basic principles of electromagnetic induction and provided a framework for further research.

In the 1850s and 1860s, James Clerk Maxwell built upon the work of Faraday and Gauss to develop a mathematical theory of electromagnetism. Maxwell's theory was based on the idea that electric and magnetic fields were not separate phenomena, but rather different aspects of the same underlying force. He developed a set of equations that described the behavior of electric and magnetic fields in space and time, which are now known as Maxwell's equations.

Maxwell's equations are a set of four partial differential equations that describe the behavior of electric and magnetic fields in the presence of electric charges and currents. The equations relate the electric and magnetic fields to each other and to electric charges and currents, and they describe the propagation of electromagnetic waves.

2.1	Historical context of Maxwell's equations . . .	4
2.2	Overview of Maxwell's equations	6
2.2.1	Faraday's law	6
2.2.2	Gauss's law	6
2.3	Applications	7

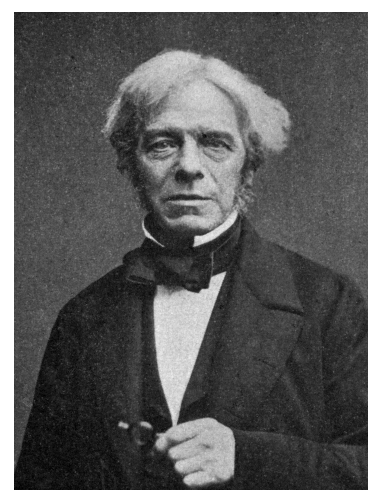


Figure 2.1: Michael Faraday (1791-1867) English scientist who made significant contributions to the fields of electromagnetism and electrochemistry. He discovered electromagnetic induction and made significant contributions to the field of electrochemistry. Despite his lack of formal education, he became one of the greatest experimentalists and theoreticians in the history of science.

Maxwell's work was not immediately recognized as a major contribution to science. At the time, the prevailing view was that electric and magnetic fields were separate phenomena. Maxwell's work showed that they were intimately related and could be described by a single set of equations. It was not until the 1880s, after Maxwell's death, that his work began to be recognized as a major contribution to science.

In the years following Maxwell's death, his work on electromagnetism was further developed by other scientists. Heinrich Hertz demonstrated the existence of electromagnetic waves in the late 1880s, and Guglielmo Marconi developed the first practical wireless telegraph in the early 1900s. Maxwell's equations also played a key role in the development of quantum mechanics and the theory of relativity.

Today, Maxwell's equations are an essential part of the study of electromagnetism and are used in many fields of science and engineering. They continue to be an active area of research, with new applications being developed all the time.

In summary, the history of electromagnetism is a story of scientific discovery and innovation, with contributions from Coulomb, Gauss, Faraday, and Maxwell. Their work has had a profound impact on our understanding of the physical world and the development of technology. The ongoing research and development of electromagnetism is a testament to its continued importance and relevance to science and engineering.

Following is a table summarizing the mentioned points:

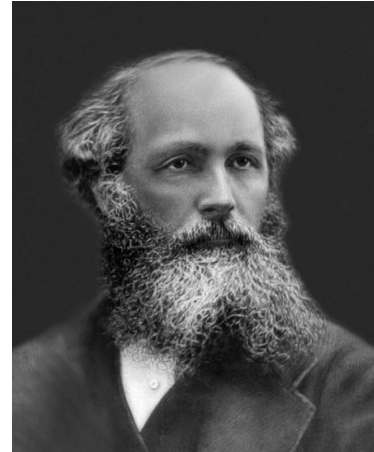
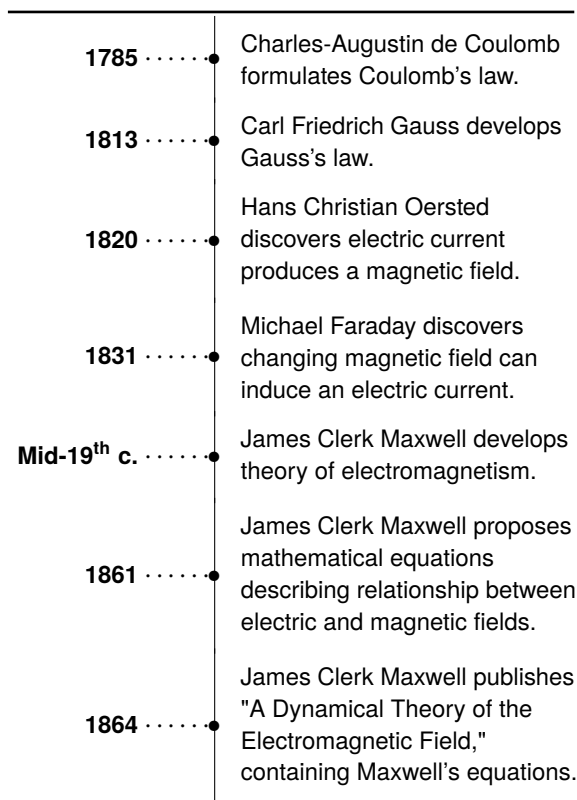


Figure 2.2: James Clerk Maxwell (1831-1879), a Scottish physicist best known for his work on electromagnetism. He developed a set of equations that described the behavior of electric and magnetic fields in space and time, known as Maxwell's equations. His work laid the foundation for the development of modern physics, including the study of electromagnetic waves and the theory of relativity. Maxwell was also a pioneer in the field of color photography and made significant contributions to the kinetic theory of gases.

Table 2.1: Key historical events leading to the establishment of Maxwell's equations

1887 • Heinrich Hertz experimentally verifies existence of electromagnetic waves.

2.2 Overview of Maxwell's equations

In the following paragraphs I will be enunciating the laws as they were first formulated. The detailed quantitative description will follow in the next chapter.

2.2.1 Faraday's law

Also known as the law of electromagnetic induction, is credited to its namesake, although it may have been anticipated by the work of Italian priest and physicist Francesco Zantedeschi in 1829 or that of Joseph Henry, who around 1830 made a similar discovery, but did not publish his findings until later.

Faraday's law of electromagnetic induction states that a changing magnetic field induces an electromotive force (EMF) in a nearby conductor, which in turn generates an electric current. In his own words, Faraday described the phenomenon in his 1831 paper "Experimental Researches in Electricity":

"If a magnetic pole be approached to a wire, it is not necessary that the wire should touch the pole, for at the moment of approximation, an electric influence or current, which is a momentary flash, is excited in the wire... Thus it appears that an electric current may be evolved from a magnetic field or force, and consequently that the influence of the magnetic force on metallic bodies takes place in obedience to some general law which also governs the evolution of electricity from magnetism."

2.2.2 Gauss's law

The second of the equations we will be considering. The law was first formulated by Joseph-Louis Lagrange in 1773, followed by Carl Friedrich Gauss in 1835, both in the context of the attraction of ellipsoids¹, which was a mathematical theorem that can be applied to vector fields.

In mathematical terms, Gauss's theorem states that the flux of a vector field through a closed surface is equal to the volume integral of the divergence of the vector field over the region enclosed by the surface.

In simpler terms, this means that the amount of a vector field passing through a closed surface is related to the way in which the vector field is changing within the volume enclosed by the surface.

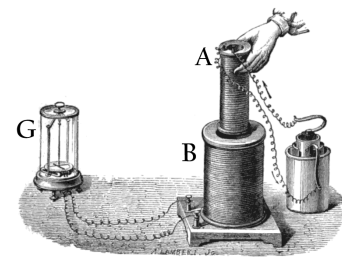


Figure 2.3: Faraday's experiment showing induction between coils of wire: The liquid battery (right) provides a current which flows through the small coil (A), creating a magnetic field. When the coils are stationary, no current is induced. But when the small coil is moved in or out of the large coil (B), the magnetic flux through the large coil changes, inducing a current which is detected by the galvanometer (G).

1: In physics and mathematics, the attraction of ellipsoids refers to the gravitational attraction between two ellipsoidal objects. The strength of the gravitational force depends on the masses of the objects and their distance apart, as well as their shapes and distributions of mass. The attraction of ellipsoids is a complex problem that requires advanced mathematical techniques to solve.

2.3 Applications

The equations, describing the most fundamental aspects of reality, are indispensable for every development field that is based on the electromagnetic phenomena.

One of the primary applications of Maxwell's equations² is in the design and analysis of electromagnetic devices. These devices include antennas, transformers, motors, and generators. By applying Maxwell's equations, engineers can predict the behavior of these devices and optimize their performance. For example, the design of an antenna for a communication system requires a detailed understanding of the propagation of electromagnetic waves. Maxwell's equations provide a framework for modeling these waves and predicting their behavior in different media, allowing engineers to design antennas that are efficient and effective.

Another concrete and personal example that led to the redaction of this dissertation is the project that was conducted under the supervision of Prof. Dr. Ing. Klaus Werner Kark, which revolved around the creation and testing of a planar multi-band antenna, also known as Bruce Array Antenna. The testing aimed to visualize and confirm the radiation patterns of said antenna vis-à-vis its theoretical model.

The software used for that work, namely CST MWS, used for the simulation of the antenna, relied heavily on discretizing the space and time in order to carry out the calculations, in a similar, albeit much more complicated fashion, to what the reader will read about in this report.

Moreover, Maxwell's equations also have important applications in the field of optics. The equations describe the behavior of electromagnetic waves, including light, which is an electromagnetic wave. Using Maxwell's equations, scientists and engineers can design optical components such as lenses, mirrors, and filters. Additionally, Maxwell's equations can be used to study the interaction of light with matter, including the absorption, reflection, and transmission of light through materials. This knowledge is essential for designing and optimizing optical devices such as lasers, fiber optic cables, and photovoltaic cells.

2: The term Maxwell's Equations will be abbreviated in the rest of this dissertation as ME

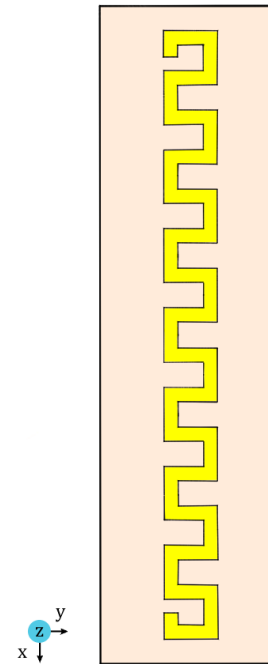
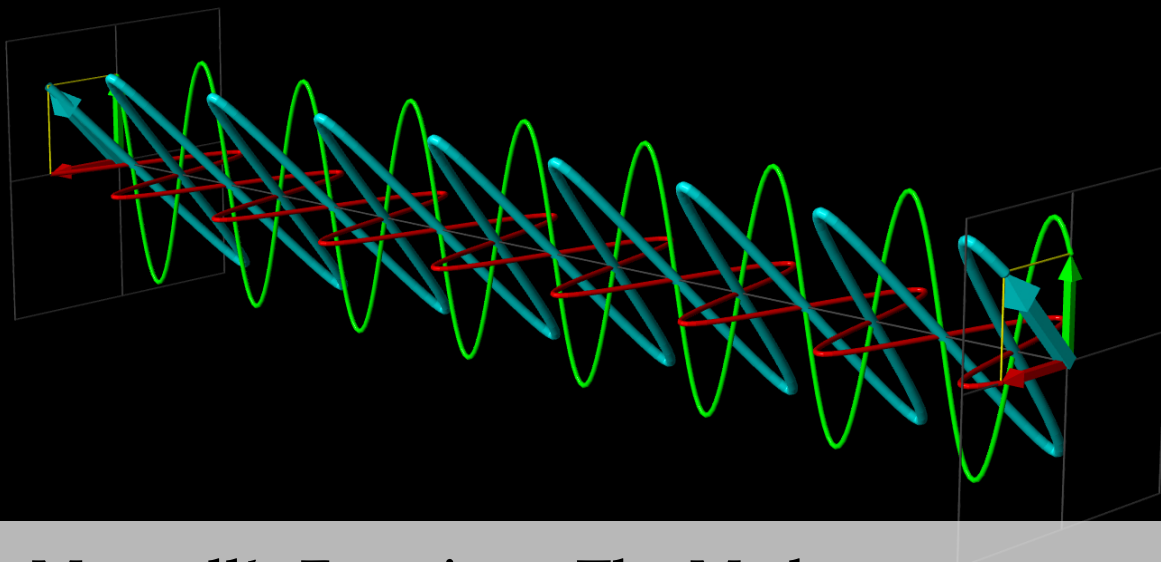


Figure 2.4: The Bruce Array Antenna design, as it is seen from the front.



3 Maxwell's Equations: The Math

This chapter delves into the cornerstone of our study: Maxwell's equations. These four partial differential equations describe the behavior of electric and magnetic fields and are essential to understanding electromagnetism. This chapter will provide a comprehensive and easy-to-understand explanation of the equations, including their physical significance. We will explore the relationship between the equations and examine the mathematical structure of the equations.

Through this chapter, we hope to provide the reader with a solid foundation for understanding the physics behind these fundamental equations.

3.1	First the basics!	8
3.1.1	A little bit of math	8
3.1.2	Coulomb's law	11
3.1.3	Electric field	12
3.1.4	Lorentz Force	13
3.1.5	Magnetic Field	13
3.1.6	Principle of charge conservation	14
3.2	The four equations	15
3.2.1	Local form	15
3.2.2	Integral form	16

3.1 First the basics!

It is beneficial to introduce a few preliminary concepts upon which the more advanced terms of MEs are built.

3.1.1 A little bit of math

We will be defining two mathematical operators while giving a small intro to the concept of operators. An operator, in this case, is a mapping¹ from \mathbb{R}^3 to a corresponding codomain. For that, we consider the vector \vec{a} , well defined and has continuous first order partial derivatives, given in Cartesian coordinates² such as

$$\vec{a}(x, y, z, t) = a_x \vec{e}_x + a_y \vec{e}_y + a_z \vec{e}_z, \quad (3.1)$$

where $a_i = f_i(x, y, z, t)$ are the scalar components alongside each of the corresponding unit vectors.

1: A mapping in mathematics is a generalization of the concept of functions from any set S_1 (called the domain) to any set S_2 (called the codomain)

2: Throughout this report, only the Cartesian coordinate system will be assumed for the vector calculus since the method used is expressed in a Cartesian-like referential. Also, the calculations in other frames are needlessly more complicated.

3.1.1.1 The divergence

Divergence (abbreviated div) is a concept in vector calculus that describes the behavior of a vector field in terms of its source or sink properties at each point in space. It measures the tendency of vector quantities, such as fluid flow or electric fields, to either converge towards or diverge from a given point.

If the divergence is positive at a particular point, it indicates a net outflow or expansion from that point. Conversely, if the divergence is negative, it signifies a net inflow or contraction.

Mathematically speaking, the divergence of the vector \vec{a} is given by

$$\operatorname{div} \vec{a} = \frac{\partial a_x}{\partial x} + \frac{\partial a_y}{\partial y} + \frac{\partial a_z}{\partial z}. \quad (3.2)$$

3.1.1.2 The curl or rotational

Curl is a mathematical operation used in vector calculus to measure the rotational behavior of a vector field. It quantifies a vector field's circulation or swirling motion around a given point.

In mathematical terms, the curl of the vector \vec{a} is given by

$$\operatorname{rot} \vec{a} = \begin{vmatrix} \vec{e}_x & \vec{e}_y & \vec{e}_z \\ \frac{\partial}{\partial x} & \frac{\partial}{\partial y} & \frac{\partial}{\partial z} \\ a_x & a_y & a_z \end{vmatrix} = \begin{bmatrix} \frac{\partial a_z}{\partial y} - \frac{\partial a_y}{\partial z} \\ \frac{\partial a_x}{\partial z} - \frac{\partial a_z}{\partial x} \\ \frac{\partial a_y}{\partial x} - \frac{\partial a_x}{\partial y} \end{bmatrix},$$

or in other terms

$$\operatorname{rot} \vec{a} = \left(\frac{\partial a_z}{\partial y} - \frac{\partial a_y}{\partial z} \right) \vec{e}_x + \left(\frac{\partial a_x}{\partial z} - \frac{\partial a_z}{\partial x} \right) \vec{e}_y + \left(\frac{\partial a_y}{\partial x} - \frac{\partial a_x}{\partial y} \right) \vec{e}_z. \quad (3.3)$$

3.1.1.3 The Nabla operator

The nabla operator (also called del) is a "symbolic vector" defined as

$$\vec{\nabla} = \frac{\partial a_x}{\partial x} \vec{e}_x + \frac{\partial a_y}{\partial y} \vec{e}_y + \frac{\partial a_z}{\partial z} \vec{e}_z. \quad (3.4)$$

Alone, it does not have much significance. However, the aforementioned operators can be rewritten in a more compact way using the nabla operator with the help of two different binary operations, namely the scalar product (\cdot) and the vector product (\times).

For instance, the re-formulation of the curl and divergence are given by the operator nabla as follows

$$\text{div } \vec{a} = \vec{\nabla} \cdot \vec{a}, \tag{3.5}$$

and

$$\text{rot } \vec{a} = \vec{\nabla} \times \vec{a}. \tag{3.6}$$

3.1.1.4 Stokes' theorem

The following two theorems are two powerful tools in vector calculus that will help deduce some results for the upcoming parts of this chapter.

Beginning with Stokes' theorem, which states that, for a closed oriented boundary Γ , delimiting a surface S_Γ whose orientation is resulting from that of Γ according to the right-hand rule³, and for the vector field \vec{a} , the following formula is valid⁴

$$\oint_{P \in \Gamma} \vec{a}(P) \cdot d\vec{l}_P = \iint_{M \in S_\Gamma} \text{rot } \vec{a}(M) \cdot d\vec{s}_M. \tag{3.7}$$

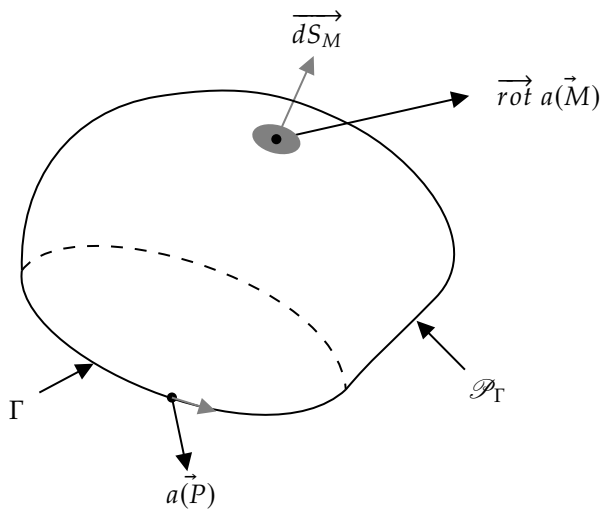


Figure 3.1: Stokes' theorem

3.1.1.5 Ostrogradsky's theorem

The second of our theorems is Ostrogradsky's theorem, also called the divergence theorem, which states that the surface integral of a vector field over a closed surface, which is called the "flux" through the surface, is equal to the volume integral of the divergence over the region inside the surface. Intuitively, it states that *the sum of all sources of the field in a region (with sinks regarded as negative sources) gives the net flux out of the region.*

In mathematical terms, let S be a closed surface⁵ and V_S the volume enclosed by said surface, the formula states that

3: By placing the right hand as in figure 3.1, the thumb gives the orientation of S_Γ and the other fingers that of Γ .

4: In the following lines, $d\tau$ and ds are infinitesimal elements of respectively the volume V and the surface S . When denotes with an under-script letter it means that the elementary entity is centered around said point.

5: Closed surfaces are oriented by defaults outwards, ie all the surface vectors are going outside of S

$$\oiint_{P \in S} \vec{a}(P) \cdot d\vec{S}_P = \iiint_{M \in V_S} \vec{\nabla} \cdot \vec{a}(M) d\tau_M. \quad (3.8)$$

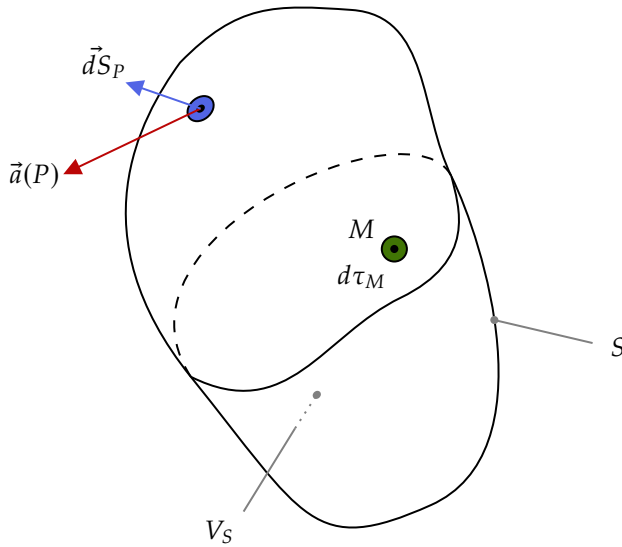


Figure 3.2: Ostrogradsky's theorem

3.1.2 Coulomb's law

The first physical concept to be discussed is Coulomb's law, which is the fundamental electromagnetic force between charged particles. It describes the interaction between two charged objects, which can be either repulsive or attractive depending on the polarity of the charges. The force is proportional to the product of the charges and inversely proportional to the square of the distance between them, as stated in Coulomb's Law. This means that the force between two charges decreases as the distance between them increases. Coulomb's force is a fundamental force in nature and plays a critical role in many phenomena, including electrostatics, electric circuits, and chemical bonding.

In mathematical terms: let there be two charged particles⁶ q_1 and q_2 at a point P such as the distance between them is r and \vec{u}_r the unitary vector from q_1 to q_2 .

6: The graphical representations of the charges are highly exaggerated for clarity reasons.

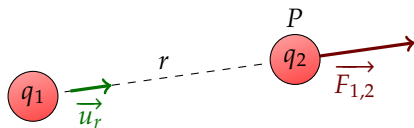


Figure 3.3: Coulomb's force of charge q_1 on charge q_2

The force exerted by 1 on 2 in the point P at the time t , said Coulomb's force is expressed as⁷

$$\vec{F}_{C_{1,2}}(P, t) = \vec{F}_C = \frac{1}{4\pi\epsilon_0} \frac{q_1 q_2}{r^2(t)} \vec{u}_r, \quad (3.9)$$

7: The space-time coordinates (M, t) (or (P, t)) shall be given in the latest form of each equation unlike with the intermediate ones where they are only assumed to avoid cluttering.

where ϵ_0 is the **permittivity of free space**, or the ability of a vacuum to permit the propagation of electric fields. Its value is approximately 8.854×10^{-12} farads per meter.

3.1.3 Electric field

The electric field is a fundamental concept in electromagnetism that describes the force experienced by a charged particle in the presence of an electric charge. It is a vector quantity that is defined as the force per unit charge at a given point in space.

As per the custom of the previous configuration, let us replace the charges q_1, q_2 and the force vector $\vec{F}_{1,2}$ with Q, q and \vec{F} respectively.⁸

8: in this case we assume both Q and q to be positive charges

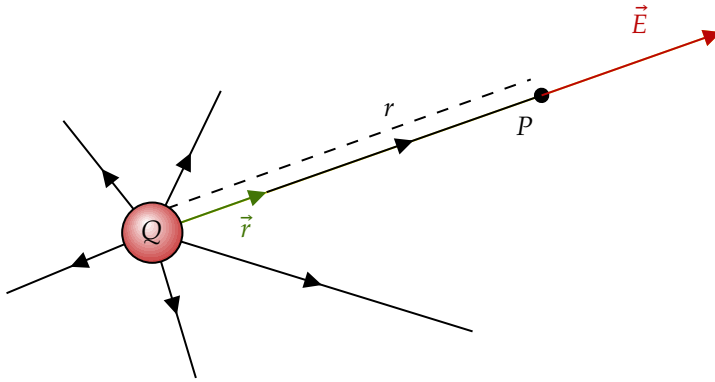


Figure 3.4: Electric field of Q with q as test charge

The electric field present at the point P is given by

$$\vec{E}(P, t) = \vec{E} = \frac{1}{q} \vec{F} = \frac{Q}{4\pi\epsilon_0 r^2(t)} \vec{u}_r. \quad (3.10)$$

Conventionally, the electric field \vec{E} at the given point P of space is considered to be in the same direction as the resulting Coulomb's force \vec{F}_p if said force is applied to a positive test charge.

However, in the real world, we seldom deal with isolated individual charges. Hence the need for an expression that takes account of the different charges present at the same time. For which a concept related to the charge is defined which is the charge density ρ at a given point M , given as

$$\rho(M, t) = \frac{dq(t)}{d\tau}, \quad (3.11)$$

for which, the expression of the electric field caused by said charge distribution in the volume V at the point P is given as

$$\vec{E}(P, t) = \vec{E}_P = \iiint_{M \in V} \frac{\rho(M(t))}{4\pi\epsilon_0 r^2(M(t))} \vec{u}_r d\tau. \quad (3.12)$$

Another formula that will be needed later throughout our report is the relation between the electric and the entity called **Electric Displacement Field** \vec{D} given as⁹

$$\vec{D}(P, t) = \epsilon_0 \vec{E}(P, t). \quad (3.13)$$

9: The complete expression is $\vec{D}(P, t) = \epsilon_0 \vec{E}(P, t) + \vec{P}$, where \vec{P} is the so-called polarization density, which will be neglected.

3.1.4 Lorentz Force

Let's consider the following graph, where the charges q_1 and q_2 are situated in the points P_1 and P_2 moving with respective speeds \vec{V}_1 and \vec{V}_2 relative to our Galilean reference frame¹⁰. In the infinitesimal time, the two charges make the elementary displacements \vec{dl}_1 and \vec{dl}_2 .

10: All movement is assumed to be happening in a Galilean reference frame

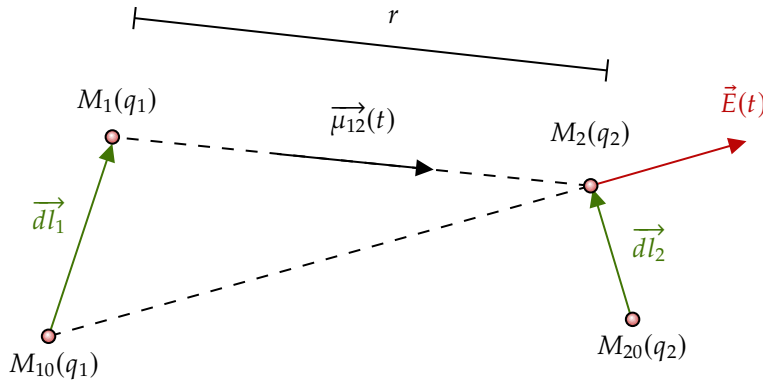


Figure 3.5: Lorentz Force

Since the force is established at a finite speed (c_0), the electric field created by q_1 at $P_{2,1}$ (the region occupied by q_2 at $t + \Delta t$) is not aligned with the vector \vec{u}_r , which means that the \vec{E} field **alone** does not explain the movement of q_2 . However, the trajectory is well accurately described if we consider the force

$$\vec{F}_{1,2}(P, t) = \frac{q_1 q_2}{4\pi\epsilon_0 r^2} \left[\vec{u}_r + \frac{\vec{V}_2(t)}{c_0} \times \left(\frac{\vec{V}_1(t)}{c_0} \times \vec{u}_r \right) \right]. \quad (3.14)$$

The resulting force is called the **Lorentz force**¹¹ which includes two terms:

11: Named after the Dutch physicist Hendrik A. Lorentz

- ▶ The term $\frac{q_1 q_2}{4\pi\epsilon_0 r^2} \vec{u}_r$ which is the electric force as we have seen before
- ▶ The second term, namely: $\frac{q_1 q_2}{4\pi\epsilon_0 r^2} \frac{\vec{V}_2}{c_0} \times \left(\frac{\vec{V}_1}{c_0} \times \vec{u}_r \right)$, which is the **magnetic force**¹².

12: Note how the magnetic force alone is responsible for the change in direction which created the discrepancy when trying to explain the trajectory with the electric force only.

We call the entity $\mu_0 = \frac{1}{\epsilon_0 c_0^2}$ the **vacuum permeability** or permeability of free space.

The magnetic force is then given by

$$\vec{F}_{B1,2}(P, t) = \vec{F}_B = \mu_0 \frac{q_1 q_2}{4\pi r^2} \vec{V}_2 \times \vec{V}_1 \times \vec{u}_r. \quad (3.15)$$

Speak about moving charge, then general when there is electrical and magnetic field, draw a similarity between electric fields and magnetic field **use resume for equation and illustration magnetic fields needs to be defined by currents, not monopoles and that the magnetic fields are resulting from moving charges, not static charges**

3.1.5 Magnetic Field

As it has been established while discussing the magnetic force, the origin of the magnetic fields are not static charges, but moving ones. And

similarly to what has been given for the electric field, the magnetic field created by the charge Q animated with the velocity \vec{V}_1 is defined henceforth as

$$\overrightarrow{B(P, t)} = \vec{B} = \mu_0 \frac{q_1}{4\pi r^2} \vec{V}_1 \times \vec{u}_r. \quad (3.16)$$

The parallels to the electric field, however, do not carry on to the volume distributions. In the case of the magnetic field, and since it is not possible to have magnetic monopoles as opposed to the singularly isolated charges which are the electric monopoles, we define the magnetic field with currents, or rather the **current density** \vec{J} ¹³ which is defined in our case as

$$\overrightarrow{J_S(M, t)} = \vec{J}_S = \sigma_m(M, t) \overrightarrow{V(M, t)}. \quad (3.17)$$

Where σ_m is the mobile surface charge. Subsequently, the expression of a magnetic field created by said current distribution is given by

$$\overrightarrow{B(P, t)} = \vec{B}_P = \iint_{M \in S} \frac{\mu_0 \overrightarrow{J_S(M, t)} dS \times \vec{u}_r}{4\pi r^2(M(t))}, \quad (3.18)$$

also referred to as the **Biot-Savart law**¹⁴.

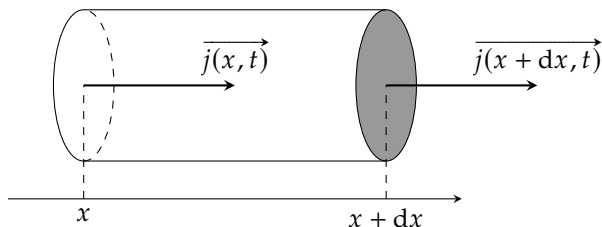
As we have done with the \vec{E} field, another quantity shall be introduced, which will be used later on. The quantity is named **magnetic field strength** and is

$$\overrightarrow{H(P, t)} = \frac{1}{\mu_0} \overrightarrow{B(P, t)}. \quad (3.19)$$

The reader should notice the independence of the two quantities, namely the electrostatic and magnetostatic fields of each other. A concept that will no longer hold once the time-dependent current and charges are introduced.

3.1.6 Principle of charge conservation

Yet another concept to understand how the ME link to each other. It states that the total electric charge in an isolated system never changes. In essence, charge conservation is an accounting relationship between the amount of charge in a region and the flow of charge into and out of that region, given by a continuity equation¹⁵ between the volumic charge density $\rho = \rho(x, t)$ and current density vector $\vec{J} = \vec{J}(x, t)$ ¹⁶.



By establishing the charge balance, ie calculating the charge that got into the volume $d\tau = Sdx$, we get

$$\frac{\partial \rho(x, t)}{\partial t} + \frac{\partial j(x, t)}{\partial x} = 0.$$

13: Among the three forms of current distribution: line, surface and volume distributions, we will focus on the second one since it is the one offering the best approximation to the real world while keeping the calculations feasible.

14: Named after the two French scientists Jean-Baptiste Biot (1774-1862) and Félix Savart (1791-1841.)

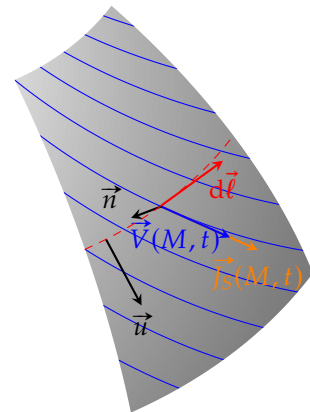


Figure 3.6: A conducting plane with a current with the current density \vec{J} (see graph opposite), parallel to the movement of charge carriers.

15: It is an equation that describes the transport of some quantity. It is particularly simple and powerful when applied to a conserved quantity such as electric charges in our case

16: We assume the distribution of current to be only x-dependent, for which feasible calculations are possible. We accept the generalization of the result.

In case of a line distribution of current $\vec{j} = \overrightarrow{j(x,t)}$ we get the famous conservation equation

$$\frac{\partial \rho}{\partial t} + \vec{\nabla} \cdot \vec{j} = 0. \quad (3.20)$$

3.2 The four equations

After laying down the key concepts involved in the definition of ME, the reader will be introduced to the equations in two steps. The first part is the exhibition of their "local" form as they are called in the contemporary literature, followed by their "integral" form which will be derived through the use of some vector calculus.

3.2.1 Local form

After having discussed the concepts of magnetic and electric fields and what revolves around them, we can safely announce the four equations as it has settled shortly after the times of James Clark Maxwell. Let M be a material point in space at the moment t , the ME are enunciated such as

$$\begin{aligned} \vec{\nabla} \cdot \overrightarrow{E(M,t)} &= \frac{\rho}{\epsilon_0}, \\ \vec{\nabla} \cdot \overrightarrow{B(M,t)} &= 0, \\ \vec{\nabla} \times \overrightarrow{E(M,t)} &= -\frac{\partial \overrightarrow{B(M,t)}}{\partial t}, \\ \vec{\nabla} \times \overrightarrow{B(M,t)} &= \mu_0 \left(\overrightarrow{j(M,t)} + \epsilon_0 \frac{\partial \overrightarrow{E(M,t)}}{\partial t} \right), \end{aligned}$$

with the relation equations

$$\begin{aligned} \vec{D} &= \epsilon_0 \vec{E}, \\ \vec{H} &= \frac{1}{\mu_0} \vec{B}, \\ \vec{j} &= \kappa \vec{E} + \rho \vec{v}. \end{aligned}$$

The equations are called -respective to their order of listing- as follows:

1. **Maxwell-Gauss (M-G)**,
2. **Maxwell-Flux (M-Φ)**,
3. **Maxwell-Faraday (M-F)** and
4. **Maxwell-Ampère (M-A)**.

The *MF* and *MA* are called the **coupling equations**. The coupling equations in Maxwell's equations describe the relationship between the changing electric and magnetic fields. They capture how a changing magnetic field induces an electric field (Faraday's law) and how a changing

electric field generates a magnetic field (Ampere's law with Maxwell's addition). These equations are crucial for understanding the interplay between electric and magnetic fields in electromagnetic phenomena.

3.2.2 Integral form

Keeping those equations in this form is pleasant to the eye. However, the numerical method used for this thesis requires multiple summations since it is the machine's way of translating the concept of integration.

In the following lines, the integral equations shall be derived from their local counterparts.

3.2.2.1 Maxwell-Gauss

On one hand, we begin with the left side of MG, applying Ostogradsky's theorem to it:

$$\begin{aligned} \iiint_V \vec{\nabla} \cdot \vec{E} \, d\tau &= \oiint_S \vec{E} \cdot \vec{ds} \\ &= \frac{1}{\epsilon_0} \iiint_V \rho \, d\tau \end{aligned} \quad (\text{MG})$$

Taking into consideration the relation equation in (3.13) we get

$$\vec{\nabla} \cdot \vec{D} = \rho$$

and deriving partially over time t ¹⁷

$$\vec{\nabla} \cdot \frac{\partial \vec{D}}{\partial t} = \frac{\partial \rho}{\partial t} \quad (*)$$

17: We accept the interchangeability between the nabla operator and the time derivative

On the other hand, by replacing (*) in the charge conservation equation the following equation¹⁸ emerges¹⁹

$$\vec{\nabla} \cdot \frac{\partial \vec{D}}{\partial t} + \vec{\nabla} \cdot \vec{j} = \vec{\nabla} \cdot \left(\frac{\partial \vec{D}}{\partial t} + \vec{j} \right) = 0, \quad (**)$$

18: Such formulation will be relevant for the computation down the line

19: The distributive property is also admitted to be true

Integrating (**) over the volume V

$$\iiint_{V_S} \vec{\nabla} \cdot \left(\frac{\partial \vec{D}}{\partial t} + \vec{j} \right) \, d\tau = \oiint_S \left(\frac{\partial \vec{D}}{\partial t} + \vec{j} \right) \vec{ds}. \quad (\text{Ostogradsky})$$

We finally get the first ME,

$$\oiint_S \left(\frac{\partial \vec{D}}{\partial t} + \vec{j} \right) \vec{ds} = 0.$$

3.2.2.2 Maxwell-Flux

The same as with MG, applying Ostogradsky to $\text{M}\Phi$ yields

$$\vec{\nabla} \cdot \vec{B} = 0 \quad \implies \iiint_{V_S} \vec{\nabla} \cdot \vec{B} \, d\tau = \oiint_S \vec{B} \cdot \vec{ds} = 0.$$

Hence the second ME equation:

$$\oiint_S \vec{B} \cdot \vec{ds} = 0 \quad (3.21)$$

3.2.2.3 Maxwell-Faraday

For this equation, we will need two identities, from one side we can establish through Stokes that

$$\iint_S \vec{\nabla} \times \vec{E} \cdot \vec{ds} = \oint_{\Gamma} \vec{E} \cdot \vec{dl}, \quad (*)$$

and applying the double integration to both sides of the MF

$$\iint_S \vec{\nabla} \times \vec{E} \cdot \vec{ds} = \iint_S -\frac{\partial \vec{B}}{\partial t} \cdot \vec{ds} \quad (**)$$

From * and ** we conclude that

$$\oint_{\Gamma} \vec{E} \cdot \vec{dl} = - \iint_S \frac{\partial \vec{B}}{\partial t} \cdot \vec{ds} \quad (3.22)$$

3.2.2.4 Maxwell-Ampère

Finally, the last equation shall be derived from the local MA, we begin by applying Stokes' to its right-hand side and adopting the relation equations

$$\iint_S \vec{\nabla} \times \vec{B} \cdot \vec{ds} = \oint_{\Gamma} \vec{B} \cdot \vec{dl} = \mu_0 \oint_{\Gamma} \vec{H} \cdot \vec{dl}, \quad (*)$$

and by double-integrating the left-hand side

$$\iint_S \mu_0 \left(\vec{j} + \epsilon_0 \frac{\partial \vec{E}}{\partial t} \right) \cdot \vec{ds} = \mu_0 \iint_S \left(\vec{j} + \epsilon_0 \frac{\partial \vec{E}}{\partial t} \right) \cdot \vec{ds} \quad (**)$$

By equating * and ** we get the integral form of the MF

$$\oint_{\Gamma} \vec{H} \cdot \vec{dl} = \iint_S \left(\vec{j} + \epsilon_0 \frac{\partial \vec{E}}{\partial t} \right) \cdot \vec{ds}, \quad (3.23)$$

the last of the four equations.

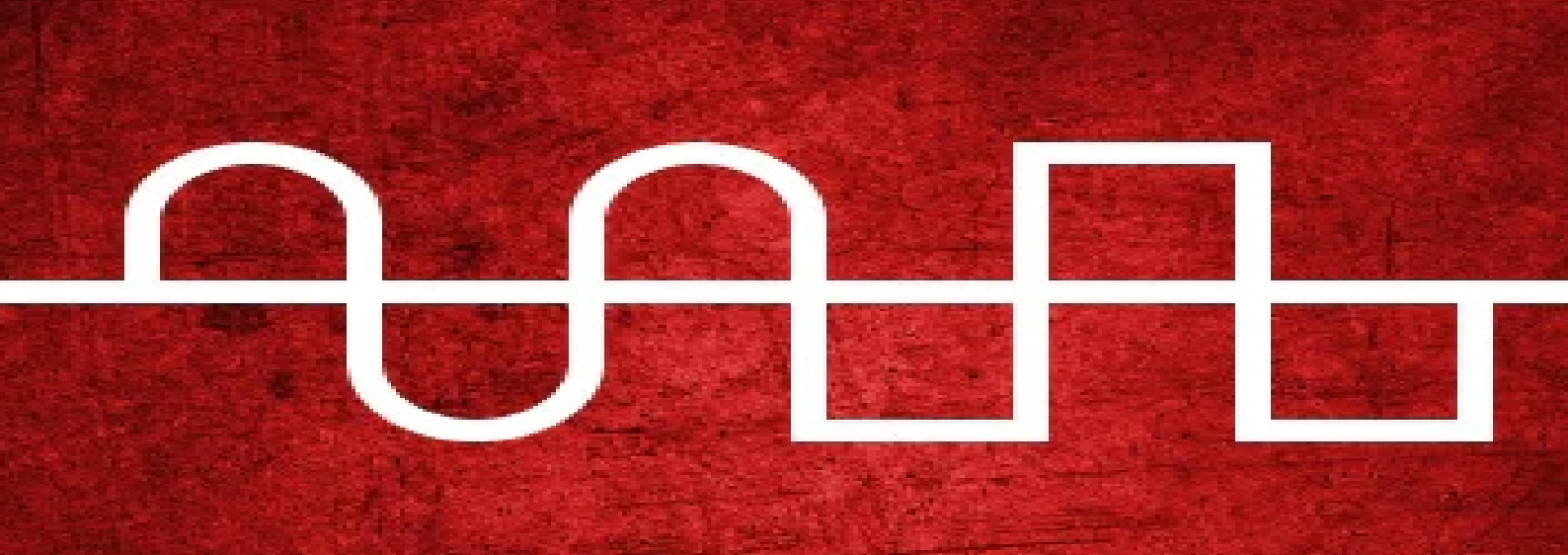
Finally, we get the famous integral equations

$$\begin{aligned} \oiint_{\mathcal{S}} \left(\frac{\partial \vec{D}}{\partial t} + \vec{j} \right) \cdot \vec{dS} &= 0 \\ \oiint_{\mathcal{S}} \vec{B} \cdot \vec{dS} &= 0 \\ \oint_{\Gamma_{\mathcal{S}}} \vec{E} \cdot \vec{dl} &= - \iint_{\mathcal{S}_T} \frac{\partial \vec{B}}{\partial t} \cdot \vec{dS} \\ \oint_{\Gamma_{\mathcal{S}}} \vec{H} \cdot \vec{dl} &= \iint_{\mathcal{S}_T} \left(\frac{\partial \vec{D}}{\partial t} + \vec{j} \right) \cdot \vec{dS} \end{aligned}$$

and

$$\begin{aligned} \vec{D} &= \epsilon_0 \vec{E} \\ \vec{H} &= \frac{1}{\mu_0} \vec{B} \\ \vec{j} &= \kappa \vec{E} + \rho \vec{v}. \end{aligned}$$

The following chapter will be exhibiting the method used in the research paper, namely the *Finite Difference Time Domain*.



4 A Numerical Approximation

Throughout this chapter, we will be addressing the computational method based on the finite difference time domain. Firstly, an introduction to the method shall take place, followed by a concrete application to our subject study, ie ME.

4.1 Defining the framework

4.1.1 So what is the FTDT?

Finite Difference Time Domain (FDTD), also known as Yee’s method, is a numerical technique used to model computational electrodynamics by approximating the associated system of differential equations. The method, named after Kane S. Yee, is particularly effective for time-domain analysis, as it allows for a single simulation run to cover a wide frequency range and handle nonlinear material properties seamlessly.

As a member of the grid-based differential numerical modeling methods, FDTD discretizes the time-dependent Maxwell’s equations using central-difference approximations for both space and time partial derivatives. The resulting finite-difference equations are then solved in either software or hardware using a leapfrog approach.

Specifically, the electric field vector components within a spatial volume are solved at a specific time step, followed by the computation of the magnetic field vector components in the same volume at the next time step. This iterative process continues until the desired transient or steady-state electromagnetic field behavior is fully captured.

4.1.2 The Yee Grid

4.1.2.1 A definition

Before establishing the discretized forms of our equations, it would be convenient to present the grid upon which such projection will take place.

- 4.1 Defining the framework . 19
- 4.1.1 So what is the FTDT? . . 19
- 4.1.2 The Yee Grid 19
- 4.2 Discretizing the equations 23
- 4.2.1 Maxwell-Faraday 23
- 4.2.2 Maxwell-Ampère 29
- 4.2.3 Maxwell-Flux 31
- 4.2.4 Maxwell-Gauss 31
- 4.2.5 Final discretized grid equation 31



Figure 4.1: Kane Shee-Gong Yee (born March 26, 1934) is a Chinese-American electrical engineer and mathematician. He is best known for introducing the finite-difference time-domain method in 1966.

The Yee grid, is a specific type of numerical grid used in the Finite-Difference Time-Domain (FDTD) method for solving Maxwell's equations. The Yee grid is designed to discretize space and time in a way that allows for accurate simulation of electromagnetic wave propagation.

This grid G can be defined mathematically in the following way where the system is an orthogonal coordinate system¹

$$G = \{(u_i, v_j, w_k); i \in \{1, \dots, I\}; j \in \{1, \dots, J\}; k \in \{1, \dots, K\}\} \quad (4.1)$$

1: The coordinate system is not necessarily orthonormal.

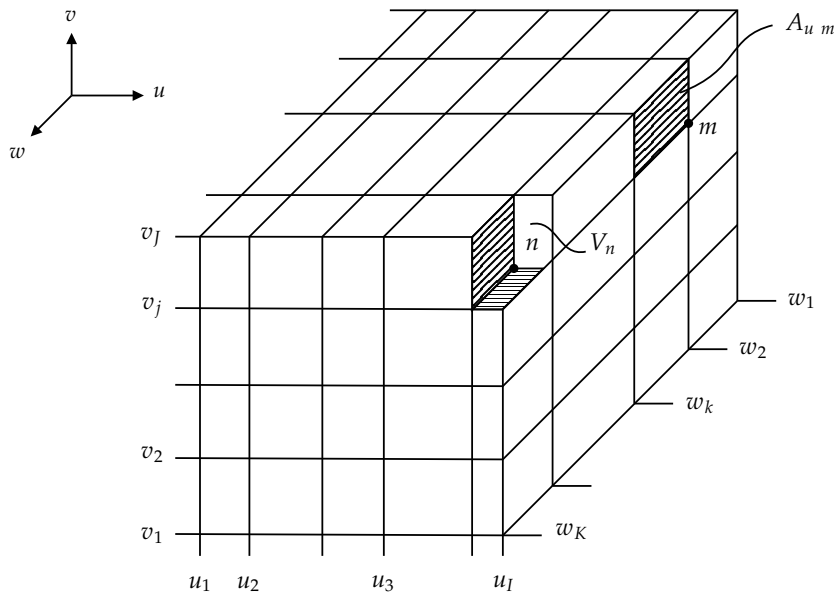


Figure 4.2: 3D Yee Grid

At each vertex of the grid G , we can define a **node** n , and with this setup, we end up with $N = I \times J \times K$ nodes. Said nodes need to be numbered.

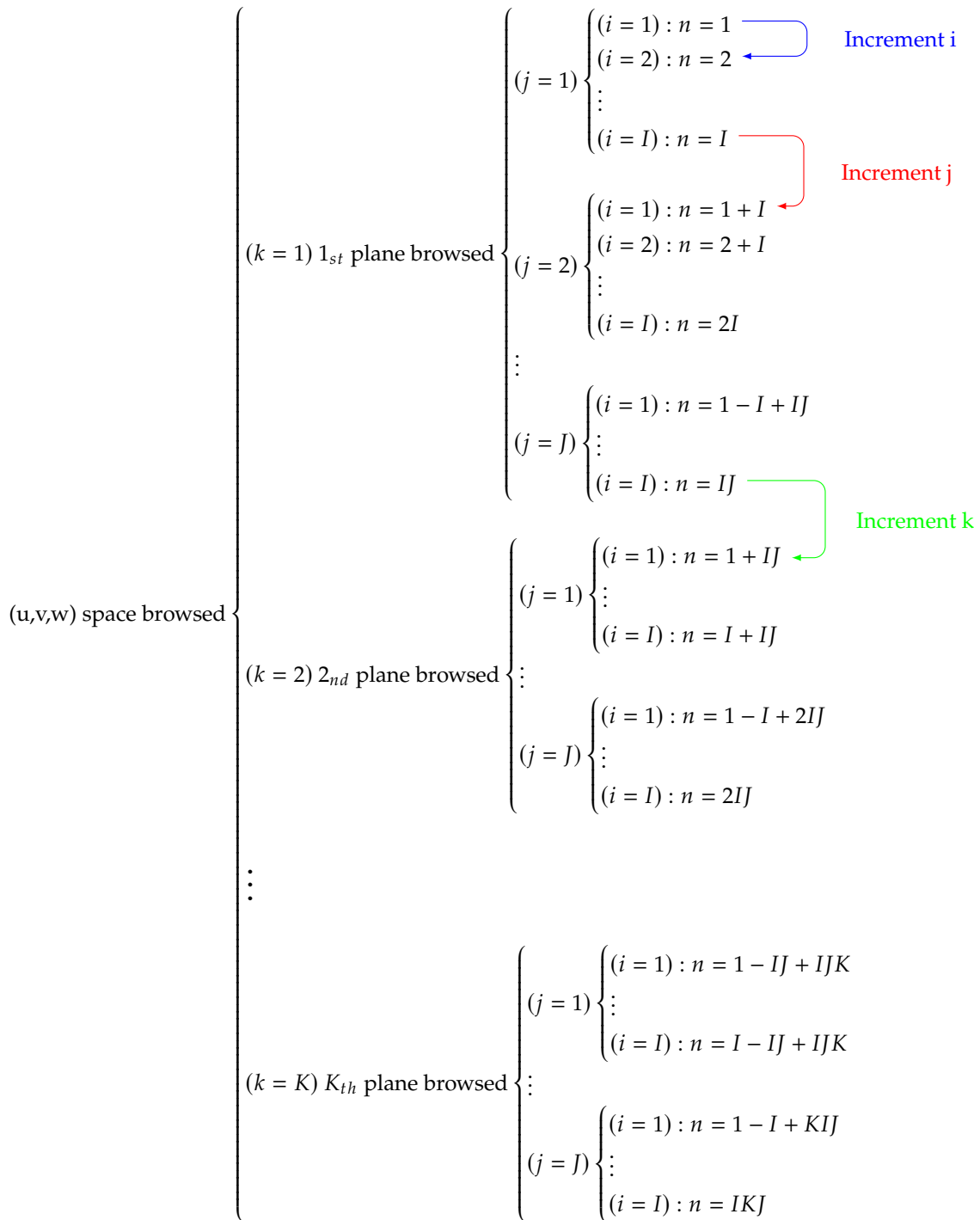
For which, and in order to stay faithful to the research paper, a linear numbering scheme shall be used instead of a 3-dimensional indexing, ie the triplet (i, j, k) .

Such numbering is given by the equation:

$$n = 1 + (i - 1)M_u + (j - 1)M_v + (k - 1)M_w \quad (4.2)$$

where² $M_u = 1$, $M_v = I$ and $M_w = I \times J$. Due to its linear pattern, following the index n might be confusing. The increment pattern can be summarized in the following tree according to the aforementioned equations as follows:

2: Other permutations are possible but for our pattern, we adopt this scheme.



Beginning from the top-right side of the tree, the index i is incremented until reaching I within the first u -axis line with the index $j = 1$. When the i set of values is browsed, then the first line is browsed. Afterward, the second u -axis line $j = 2$ is to be browsed. The process goes on until every single u -axis line is covered. This whole process happens within the first plane (u, v) defined by $I \times J$ nodes. The same nested process is repeated for each value of k which assures by the end of the process the whole grid, ie the space (u, v, w) to be enumerated.

4.1.2.2 Advantages of the Yee Grid

Before delving into the matter, there needs to be a talk about a more intuitive grid setup for the vectors in question as a comparison. The intuitive way of arranging the vector components of \vec{E} and \vec{H} fields is to superpose them atop each other on each axis accordingly, ie using what is called *co-located grid*. The following setup is then realized:

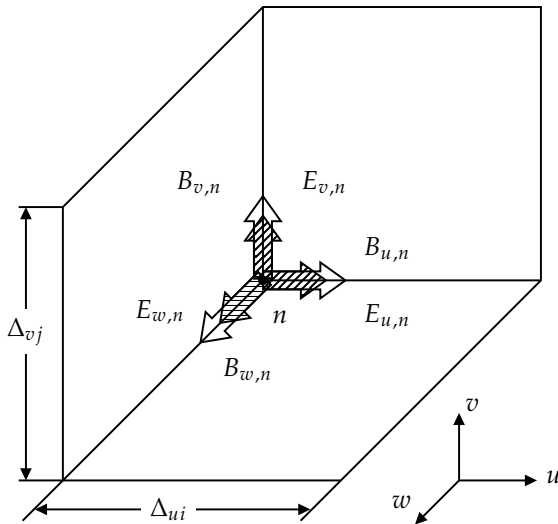


Figure 4.3: A co-located grid

Despite being more intuitive, this arrangement proves to be inconvenient for the purposes of our method. A parallel shall be drawn when compared to its co-located counterpart.

The other, less intuitive setup is what is conventionally called a staggered grid, which consists of allocating electric field components to the middle of the vertices connected to the node in question, while the magnetic field components are located at the center of each grid cell face as shown in the graph below:

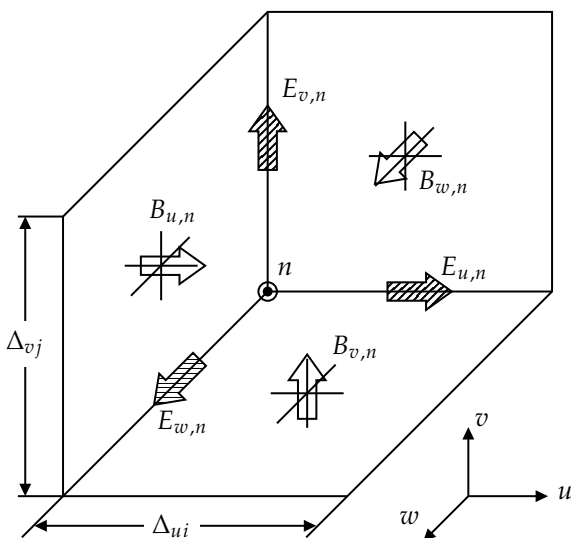


Figure 4.4: A staggered grid

The staggered Yee grid is designed to minimize numerical artifacts

and provide better accuracy. In this grid, the electric field components ($E_{u,n}, E_{v,n}, E_{w,n}$) are positioned at the vertices of the grid cells, while the magnetic field components ($B_{u,n}, B_{v,n}, B_{w,n}$) are located on the faces of the grid. This staggered arrangement ensures proper spatial and temporal alignment between the fields, leading to more accurate calculations of field interactions and wave propagation.

On the other hand, the normal co-located grid places both electric and magnetic field components superposed at each node on the three axes. This arrangement simplifies the data storage and access but may introduce some numerical errors, especially when capturing electromagnetic wave phenomena accurately.

To illustrate the differences between the two grid configurations, we present a comparison table:

Grid Configuration	Advantages	Disadvantages
Staggered Yee grid	<ol style="list-style-type: none"> 1. Accurate field interactions and propagation. 2. Reduced numerical artifacts. 	<ol style="list-style-type: none"> 1. Requires special interpolation for sources. 2. More complex data storage and access.
Normal co-located grid	<ol style="list-style-type: none"> 1. Simpler data storage and access. 2. Easier implementation for simpler problems. 	<ol style="list-style-type: none"> 1. Easier implementation for simple problems. 2. Less accurate for capturing wave phenomena.

Figure 4.5: Comparison between staggered and co-located grid

4.2 Discretizing the equations

The integral forms of ME, being expressed as an integral, are equivalent to successive additions. As a first step, the discretization of a single equation shall be provided, followed by the descriptive matrices of the entirety of the studied propagation volume.

The reader should notice that in this dissertation, the entities on the left-hand side are considered *causes* while those on the right are their corresponding *effects*. The setup becomes then understandable since it represents the *cause-effect* relationship between the \vec{E} and \vec{B} fields in a more natural manner.

4.2.1 Maxwell-Faraday

We shall begin with the first coupling equation, namely MF:

$$\oint_{\Gamma_S} \vec{E} \cdot \vec{dl} = - \iint_{S_r} \frac{\partial \vec{B}}{\partial t} \cdot \vec{dS}$$

On one hand, we consider the left-hand side of the equation. The integral along the border of an elementary cell is carried out according to the following scheme:

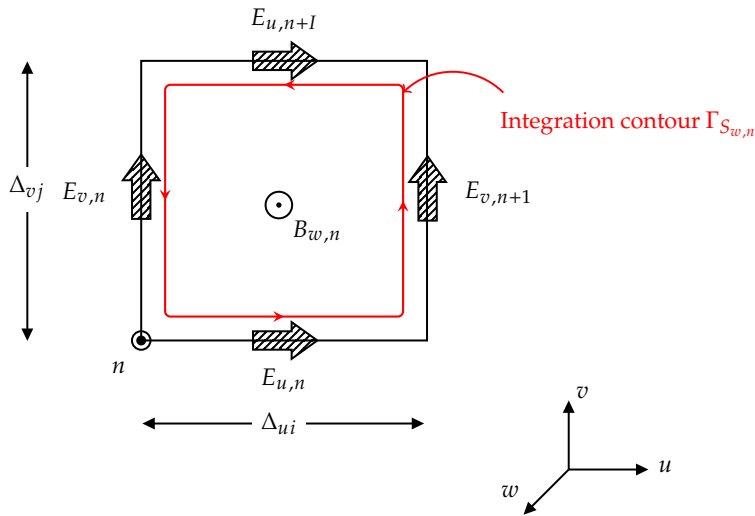


Figure 4.6: Elementary cell integration scheme

According to the trapezoidal rule³, where $\Delta_{ui} = u_{i+1} - u_i$ and $\Delta_{vj} = v_{j+1} - v_j$ we get⁴:

$$\oint_{\Gamma_{S_{w,n}}} \vec{E} \cdot \vec{dl} = (u_{i+1} - u_i)E_{u,n} + (v_{j+1} - v_j)E_{v,n+1} + (u_{i+1} - u_i)E_{u,n+1} + (v_{j+1} - v_j)E_{v,n} + \mathcal{O}[(u_{i+1} - u_i)^2] + \mathcal{O}[(v_{j+1} - v_j)^2] \tag{4.3}$$

3: Called in the paper the *first order integration formula*

4: The term $\Gamma_{S_{w,n}}$ designates the contour Γ resting on the area $S_{w,n}$ such as it is associated with the node n and having the field component $B_{w,n}$ in its midst.

The *big O* notation suggests the absolute value of the error of the circulation of the E field with its discretized expression is at most some linear combination of $(u_{i+1} - u_i)^2$ and $(v_{j+1} - v_j)^2$ when the cell dimensions tend to 0.

On the other hand, let's consider the graphic below

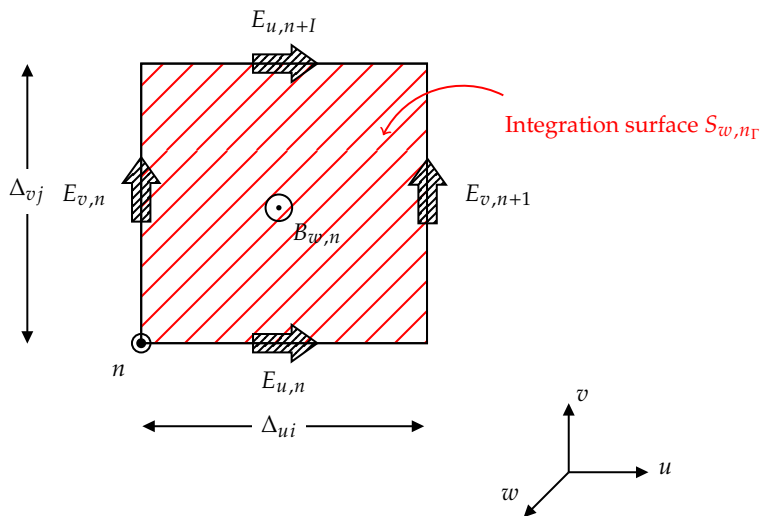


Figure 4.7: Elementary cell integration surface

Applying the same principle to the right-hand side yields the following expression

$$\iint_{S_{w,n\Gamma}} \frac{\partial \vec{B}}{\partial t} \cdot \vec{dS} = \dot{B}_{w,n}(u_{i+1} - u_i)(v_{j+1} - v_j) + \mathcal{O} \left[((u_{i+1} - u_i)(v_{j+1} - v_j))^2 \right]. \quad (4.4)$$

Equating equations (4.3) and (4.4) we get the first discrete replacement for the M-F equation: add mention of get rid of approximation term

$$(u_{i+1} - u_i)E_{u,n} + (v_{j+1} - v_j)E_{v,n+1} + (u_{i+1} - u_i)E_{u,n+1} + (v_{j+1} - v_j)E_{v,n} = \dot{B}_{w,n}(u_{i+1} - u_i)(v_{j+1} - v_j). \quad (4.5)$$

However, this equation concerns a single surface area out of three surface areas associated with a single node, namely n . If we are to describe the whole structure, we will need a set of $3 \times N$ equations. In order to achieve this, we shall adopt the matrix notation, which offers a condensed form for equation management.

Practically speaking, if we consider the M-F equation:

$$\oint_{\Gamma_S} \vec{E} \cdot \vec{dl} = - \iint_{S_\Gamma} \frac{\partial \vec{B}}{\partial t} \cdot \vec{dS}$$

For each highlighted component in the equation, a matrix (operation of matrices) shall be provided.

4.2.1.1 Expression of the contour integral

A first step preceding the establishment of the contour integral matrix is the introduction of three discretization matrices, each one for one of the node's faces.

- The first matrix is given by

$$(P_u)_{m,p} = \begin{cases} -1, & \text{for } rp = m \\ 1, & \text{for } p = m + M_u = m + 1 \text{ where: } (m, p) \in \llbracket 1, N \rrbracket^2 \\ 0, & \text{elsewhere} \end{cases} \quad (4.6)$$

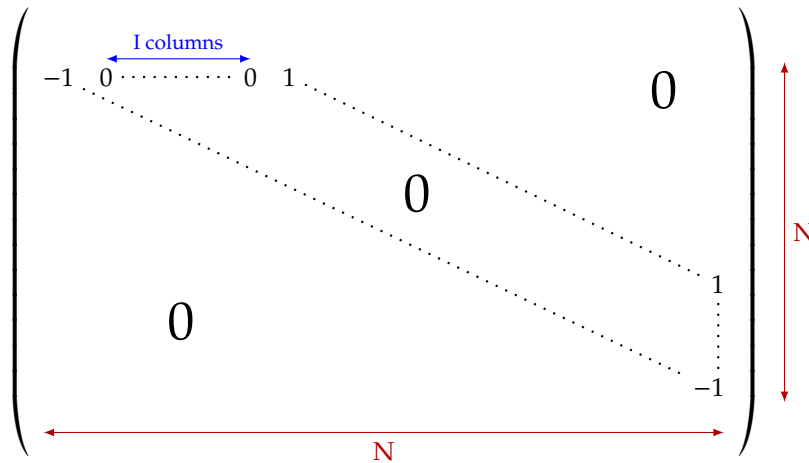
which yields the following matrix form

$$\begin{pmatrix} -1 & 1 & 0 & \dots & 0 \\ 0 & -1 & 1 & \dots & 0 \\ 0 & 0 & -1 & \ddots & \vdots \\ \vdots & \vdots & \ddots & \ddots & 1 \\ 0 & 0 & \dots & 0 & -1 \end{pmatrix}$$

► Similarly, the second matrix

$$(P_v)_{m,p} = \begin{cases} -1, & \text{for } p = m \\ 1, & \text{for } p = m + M_v = m + I \text{ where: } (m, p) \in \llbracket 1, N \rrbracket^2 \\ 0, & \text{elsewhere} \end{cases} \quad (4.7)$$

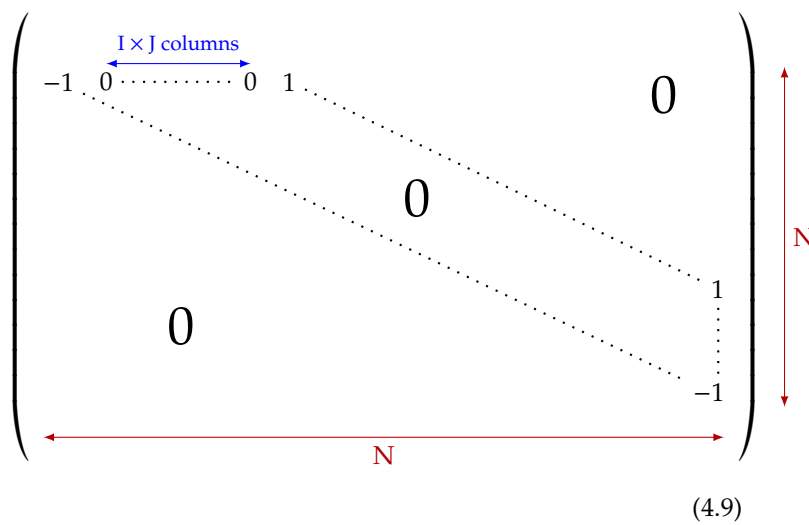
which results in



► In the same manner we get the third matrix

$$(P_w)_{m,p} = \begin{cases} -1, & \text{for } p = m \\ 1, & \text{for } p = m + M_w = m + I \times J \text{ where: } (m, p) \in \llbracket 1, N \rrbracket^2 \\ 0, & \text{elsewhere} \end{cases} \quad (4.8)$$

which results in



The 3 matrices are to be combined into an even bigger matrix, which represents the topological part of the contour integral (curl), \mathbf{C} , with a dimension of $3N \times 3N$, such as

$$\begin{pmatrix}
 \mathbf{0} & \begin{array}{c} \text{---}P_w \\ \begin{array}{|c|} \hline \begin{array}{ccc} 1 & \text{---} & -1 & 0 \\ & \diagdown & & \\ & & 0 & -1 \\ & & & \vdots \\ 0 & & & 1 \end{array} \\ \hline \end{array} \end{array} & \begin{array}{c} P_v \\ \begin{array}{|c|} \hline \begin{array}{ccc} -1 & \text{---} & 1 & 0 \\ & \diagdown & & \\ & & 0 & 1 \\ & & & \vdots \\ 0 & & & -1 \end{array} \\ \hline \end{array} \end{array} \\
 \begin{array}{c} P_w \\ \begin{array}{|c|} \hline \begin{array}{ccc} -1 & \text{---} & 1 & 0 \\ & \diagdown & & \\ & & 0 & 1 \\ & & & \vdots \\ 0 & & & -1 \end{array} \\ \hline \end{array} \end{array} & \mathbf{0} & \begin{array}{c} \text{---}P_u \\ \begin{array}{|c|} \hline \begin{array}{ccc} 1 & -1 & & 0 \\ & \diagdown & & \\ & & & \vdots \\ 0 & & & -1 \\ & & & 1 \end{array} \\ \hline \end{array} \end{array} \\
 \begin{array}{c} \text{---}P_v \\ \begin{array}{|c|} \hline \begin{array}{ccc} 1 & \text{---} & -1 & 0 \\ & \diagdown & & \\ & & 0 & -1 \\ & & & \vdots \\ 0 & & & 1 \end{array} \\ \hline \end{array} \end{array} & \begin{array}{c} P_u \\ \begin{array}{|c|} \hline \begin{array}{ccc} 1 & -1 & & 0 \\ & \diagdown & & \\ & & & \vdots \\ 0 & & & -1 \\ & & & 1 \end{array} \\ \hline \end{array} \end{array} & \mathbf{0}
 \end{pmatrix}$$

4.2.1.2 Expression of the electromagnetic fields

The unknown field components of the different fields will be stored accordingly in vectors of dimension $3N$.

- The \vec{E} , \vec{D} , \vec{B} , \vec{H} and \vec{J} field components are to be stored respectively in the vectors \mathbf{e} , \mathbf{d} , \mathbf{b} , \mathbf{h} and \mathbf{j} such as

$$\mathbf{e} = \begin{bmatrix} E_{u,1} \\ E_{u,2} \\ \vdots \\ E_{w,N} \end{bmatrix}; \quad \mathbf{d} = \begin{bmatrix} D_{u,1} \\ D_{u,2} \\ \vdots \\ D_{w,N} \end{bmatrix}; \quad \mathbf{b} = \begin{bmatrix} B_{u,1} \\ B_{u,2} \\ \vdots \\ B_{w,N} \end{bmatrix}; \quad \mathbf{h} = \begin{bmatrix} H_{u,1} \\ H_{u,2} \\ \vdots \\ H_{w,N} \end{bmatrix}; \quad \text{and} \quad \mathbf{j} = \begin{bmatrix} J_{u,1} \\ J_{u,2} \\ \vdots \\ J_{w,N} \end{bmatrix},$$

4.2.1.3 Length of the integration path

The integration path matrix, where the different integration paths are stored, is given by

satisfies

$$CD_s e = -D_A \dot{b} \quad (4.16)$$

4.2.2 Maxwell-Ampère

The peculiar set up of the magnetic and electric components within the grid G gives rise to a conjugal, called a *dual grid*, named \tilde{G} . Such a grid can be, akin to the grid G , be defined such as

$$\tilde{G} = \{(\tilde{u}_i, \tilde{v}_j, \tilde{w}_k); i \in \{1, \dots, I\}; j \in \{1, \dots, J\}; k \in \{1, \dots, K\}\}, \quad (4.17)$$

where

$$\left\{ \begin{array}{l} \tilde{u}_i = \frac{u_{i+1} + u_i}{2}, \quad \left\{ \begin{array}{l} i \in \{1, \dots, I-1\} \\ \tilde{u}_I = 0, \end{array} \right. \\ \tilde{v}_j = \frac{v_{j+1} + v_j}{2}, \quad \left\{ \begin{array}{l} j \in \{1, \dots, J-1\} \\ \tilde{v}_J = 0, \end{array} \right. \\ \tilde{w}_k = \frac{w_{k+1} + w_k}{2}, \quad \left\{ \begin{array}{l} k \in \{1, \dots, K-1\} \\ \tilde{w}_K = 0. \end{array} \right. \end{array} \right. \quad (4.18)$$

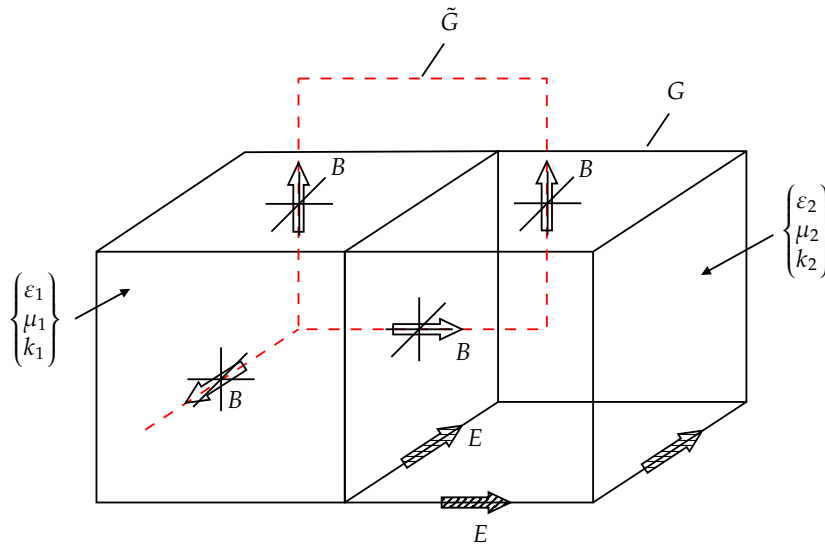


Figure 4.8: The dual grid \tilde{G}

Similarly to what has been done with first M-E, the following matrices are defined:

- The integration path length defines a matrix \tilde{D}_I :

$$(\tilde{D}_\kappa)_{2N+n} = \frac{A_{w,n-M_u} \kappa_{w,n-M_u} + A_{w,n-M_v} \kappa_{w,n-M_v} + A_{w,n} \kappa_{w,n} + A_{w,n-M_u-M_v} \kappa_{w,n-M_u-M_v}}{4\tilde{A}_{w,n}}. \quad (4.26)$$

Incidentally, we can define the relation equations such as

$$\mathbf{b} = D_\mu \mathbf{h}, \quad (4.27)$$

$$\mathbf{d} = \tilde{D}_\epsilon \mathbf{e} \quad (4.28)$$

and

$$\mathbf{j} = \tilde{D}_\kappa \mathbf{e} + D_\rho \mathbf{v}. \quad (4.29)$$

Finally we get the second discretized equation, aka the discretized M-A equation

$$\tilde{C} \tilde{D}_s D_\mu^{-1} \mathbf{b} = \tilde{D}_A (\mathbf{d} + \mathbf{j}) \quad (4.30)$$

4.2.3 Maxwell-Flux

For this part, we shall need the discretized definition of the *div* operator on G as

$$\mathbf{S} = (P_u, P_v, P_w) \quad (4.31)$$

for which we obtain the third equation

$$S D_A \mathbf{b} = \mathbf{0} \quad (4.32)$$

4.2.4 Maxwell-Gauss

For this equation, the equivalent to the matrix \mathbf{S} for the grid G is needed. Its expression is linked to its counterpart such as

$$\tilde{\mathbf{S}} = (P_u^\top, P_v^\top, P_w^\top). \quad (4.33)$$

Hence, the final M-E

$$\tilde{S} \tilde{D}_A (\mathbf{d} + \mathbf{j}) = \mathbf{0} \quad (4.34)$$

4.2.5 Final discretized grid equation

Having exhibited the origin of the discretized equations, we can lay them down elegantly in the following table:

Analog equations	Discretized equivalent
$\oint_S \left(\frac{\partial \vec{D}}{\partial t} + \vec{j} \right) \cdot \vec{dS} = 0$	$\tilde{S} \tilde{D}_A (\dot{d} + j) = 0$
$\oint_S \vec{B} \cdot \vec{dS} = 0$	$S D_A \mathbf{b} = 0$
$\oint_{\Gamma_S} \vec{H} \cdot \vec{dl} = \iint_{S_r} \left(\frac{\partial \vec{D}}{\partial t} + \vec{j} \right) \cdot \vec{dS}$	$\tilde{C} \tilde{D}_s D_\mu^{-1} \mathbf{b} = \tilde{D}_A (\dot{d} + j)$
$\oint_{\Gamma_S} \vec{E} \cdot \vec{dl} = - \iint_{S_r} \frac{\partial \vec{B}}{\partial t} \cdot \vec{dS}$	$C D_s e = -D_A \dot{\mathbf{b}}$
$\vec{D} = \epsilon_0 \vec{E}$	$\mathbf{b} = D_\mu \mathbf{h}$
$\vec{H} = \frac{1}{\mu_0} \vec{B}$	$d = \tilde{D}_\epsilon e$
$\vec{j} = \kappa \vec{E} + \rho \vec{v}$	$j = \tilde{D}_\kappa e + D_\rho v$

Figure 4.9: Conversion between analog and discretized M-Es

In the following chapter, a practical method shall be devised to tackle a simplified version of this problem.

5 Creation and Testing of a Simplified FDTD Algorithm

5.1 The code

In order to simulate what has been theoretically introduced in the last chapter, a short code shall be implemented. The code sets up the simulation environment, declares a variable Hz that will be plotted and provides a plot of the magnitude of said variable either at different time stamps or at the very end of the simulation.

5.1 The code	33
5.2 Result of the Simulation	37

```
1
2 % Parameters
3 c = 299792458; % Speed of light in m/s
4 dx = 0.01; % Spatial step size (grid spacing) in meters
5 dy = dx; % Use the same step size for y-direction
6
7 % Material properties
8 epsilon_r = 1.0; % Relative permittivity (modify for different materials)
9 mu_r = 1.0; % Relative permeability (modify for different materials)
10
11 % Initialization
12 Ex = zeros(num_points_x, num_points_y); % x-component of electric field
13 Ey = zeros(num_points_x, num_points_y); % y-component of electric field
14 Hz = zeros(num_points_x, num_points_y); % z-component of magnetic field
```

The second chunk of the code, namely the following code snippet

```
1 % Calculate maximum wave speed for CFL condition
2 v_max = 1/sqrt(epsilon_r * mu_r);
3 dt = dx / (2 * v_max); % Temporal step size to satisfy the CFL condition
```

sets up the CFL condition to be held. CFL (*Courant–Friedrichs–Lewy*). It delineates an upper limit on the size of time increments, determined by factors such as grid spacing, wave propagation speed, and the overall simulation duration.

In our context, adherence to the CFL condition guarantees that a wave-front encompasses each grid cell during a single time step. This precautionary measure averts numerical instability and fosters dependable propagation of electromagnetic fields

```

1 % Simulation parameters
2 num_steps = 400; % Number of time steps
3 num_points_x = 100; % Number of spatial points in x-direction
4 num_points_y = 100; % Number of spatial points in y-direction
5 source_position_x = floor(num_points_x / 4); % x-position of the source (excitation)
6 source_position_y = floor(num_points_y / 2); % y-position of the source (excitation)

```

Integrating a Perfectly Matched Layer (PML) into the code offers the advantage of effectively reducing reflections at the domain edges. This results in more accurate modeling of unbounded regions, minimizing artifacts and enhancing the fidelity of wave interactions.

```

1 % Perfectly Matched Layer (PML) parameters (absorbing boundary)
2 pml_thickness = 10; % Number of PML layers near the boundary
3 sigma_max = 0.1; % Maximum conductivity in the PML
4
5 % PML variables (x-direction)
6 sigma_x = zeros(num_points_x, num_points_y);
7 kappa_x = ones(num_points_x, num_points_y);
8 alpha_x = ones(num_points_x, num_points_y);
9
10 % PML variables (y-direction)
11 sigma_y = zeros(num_points_x, num_points_y);
12 kappa_y = ones(num_points_x, num_points_y);
13 alpha_y = ones(num_points_x, num_points_y);
14
15 % Calculate PML parameters
16 for i = 1:pml_thickness
17     sigma_x(i, :) = ((pml_thickness - i) / pml_thickness) ^ 3 * sigma_max;
18     sigma_x(num_points_x - i + 1, :) = ((pml_thickness - i) / pml_thickness) ^ 3 *
        sigma_max;
19     kappa_x(i, :) = 1 + ((pml_thickness - i) / pml_thickness) ^ 2 * (sigma_max / (c *
        dx));
20     kappa_x(num_points_x - i + 1, :) = 1 + ((pml_thickness - i) / pml_thickness) ^ 2 *
        (sigma_max / (c * dx));
21     alpha_x(i, :) = exp(-((sigma_x(i, :) ./ kappa_x(i, :)) + sigma_max) * dt);
22     alpha_x(num_points_x - i + 1, :) = exp(-((sigma_x(num_points_x - i + 1, :) ./
        kappa_x(num_points_x - i + 1, :)) + sigma_max) * dt);
23
24     sigma_y(:, i) = ((pml_thickness - i) / pml_thickness) ^ 3 * sigma_max;
25     sigma_y(:, num_points_y - i + 1) = ((pml_thickness - i) / pml_thickness) ^ 3 *
        sigma_max;
26     kappa_y(:, i) = 1 + ((pml_thickness - i) / pml_thickness) ^ 2 * (sigma_max / (c *
        dy));
27     kappa_y(:, num_points_y - i + 1) = 1 + ((pml_thickness - i) / pml_thickness) ^ 2 *
        (sigma_max / (c * dy));
28     alpha_y(:, i) = exp(-((sigma_y(:, i) ./ kappa_y(:, i)) + sigma_max) * dt);
29     alpha_y(:, num_points_y - i + 1) = exp(-((sigma_y(:, num_points_y - i + 1) ./
        kappa_y(:, num_points_y - i + 1)) + sigma_max) * dt);
30 end

```

From here onward, the code will be updating the components we have created, storing the resulting data and plotting the respective simulation result.

```

1 % Time-stepping loop
2 for t = 1:num_steps
3     % Update magnetic field
4     for i = 1:num_points_x-1

```

```

5     for j = 1:num_points_y-1
6         Hz(i, j) = Hz(i, j) + (Ex(i, j + 1) - Ex(i, j) - Ey(i + 1, j) + Ey(i, j))
          * dt / dx;
7     end
8 end
9
10 % Apply a more accurate Gaussian pulse as the source
11 pulse_amplitude = 1.0; % Adjust this value to control the initial pulse amplitude
12 pulse_width = 20; % Adjust this value to control the pulse width
13 pulse_decay_factor = 0.95; % Adjust this value to control the decay of the pulse
    over time
14
15 % Calculate the Gaussian pulse at the current time step with attenuation
16 pulse = pulse_amplitude * exp(-0.5 * ((t*dt - source_position_x*dx) / pulse_width
    )^2 + ((t*dt - source_position_y*dy) / pulse_width)^2));
17 pulse = pulse * pulse_decay_factor^(t-1); % Apply the time attenuation factor
18
19 % Add the pulse to the magnetic field Hz and electric field Ex
20 Hz(source_position_x, source_position_y) = Hz(source_position_x, source_position_y
    ) + pulse;
21 Ex(source_position_x, source_position_y) = Ex(source_position_x, source_position_y
    ) + pulse;
22 Ey(source_position_x, source_position_y) = Ey(source_position_x, source_position_y
    ) + pulse;
23
24 % Update electric fields with PML (x-direction)
25 for i = 2:num_points_x
26     for j = 1:num_points_y
27         Ex(i, j) = alpha_x(i, j) .* Ex(i, j) + (Hz(i, j) - Hz(i - 1, j)) * dt / (
    dx * kappa_x(i, j));
28     end
29 end
30
31 % Update electric fields with PML (y-direction)
32 for i = 1:num_points_x
33     for j = 2:num_points_y
34         Ey(i, j) = alpha_y(i, j) .* Ey(i, j) - (Hz(i, j) - Hz(i, j - 1)) * dt / (
    dy * kappa_y(i, j));
35     end
36 end
37
38 % Visualization
39 if mod(t, 10) == 0
40     figure(1);
41     imagesc((1:num_points_x)*dx, (1:num_points_y)*dy, Hz');
42     title(['Time Step: ', num2str(t)]);
43     xlabel('X (m)');
44     ylabel('Y (m)');
45     colorbar;
46     axis equal;
47     drawnow;
48 end
49 end
50
51 % Visualization of the final magnetic field
52 figure(2);
53 imagesc(Hz);
54 title('Magnetic Field (Hz)');

```

```

55 xlabel('X');
56 ylabel('Y');
57 colorbar;
58
59
60 % Center position for field visualization
61 center_x = floor(num_points_x / 2);
62 center_y = floor(num_points_y / 2);
63
64 % Arrays to store field values at the center over time
65 Hz_center = zeros(1, num_steps);
66
67 % Time-stepping loop
68 for t = 1:num_steps
69
70
71     % Store magnetic field value at the center with attenuation
72     pulse = pulse_amplitude * exp(-0.5 * ((t*dt - center_x*dx) / pulse_width)^2 + ((t
73     *dt - center_y*dy) / pulse_width)^2));
74     pulse = pulse * pulse_decay_factor^(t-1); % Apply the time attenuation factor
75     Hz_center(t) = Hz(center_x, center_y) + pulse;
76
77     % Visualization
78     if mod(t, 10) == 0
79         figure(1);
80         imagesc((1:num_points_x)*dx, (1:num_points_y)*dy, Hz');
81         title(['Time Step: ', num2str(t)]);
82         xlabel('X (m)');
83         ylabel('Y (m)');
84         colorbar;
85         axis equal;
86         drawnow;
87     end
88 end
89
90 % Visualization of the final magnetic field
91 figure(2);
92 imagesc(Hz);
93 title('Magnetic Field (Hz)');
94 xlabel('X');
95 ylabel('Y');
96 colorbar;
97
98 % Plot H field at the center as a function of time
99 figure(3);
100 time_axis = (0:num_steps-1) * dt;
101 plot(time_axis, Hz_center);
102 title('Magnetic Field (Hz) at Center');
103 xlabel('Time (s)');
104 ylabel('Magnetic Field (Hz) at Center');
105
106 % Add axis labels and units to the 2D graph
107 figure(2);
108 x_label_vals = linspace(0, num_points_x, 5);
109 x_ticks = linspace(1, num_points_x, 5);
110 y_label_vals = linspace(0, num_points_y, 5);
111 y_ticks = linspace(1, num_points_y, 5);
112 x_tick_labels = sprintfc('%.2f', x_label_vals*dx);

```

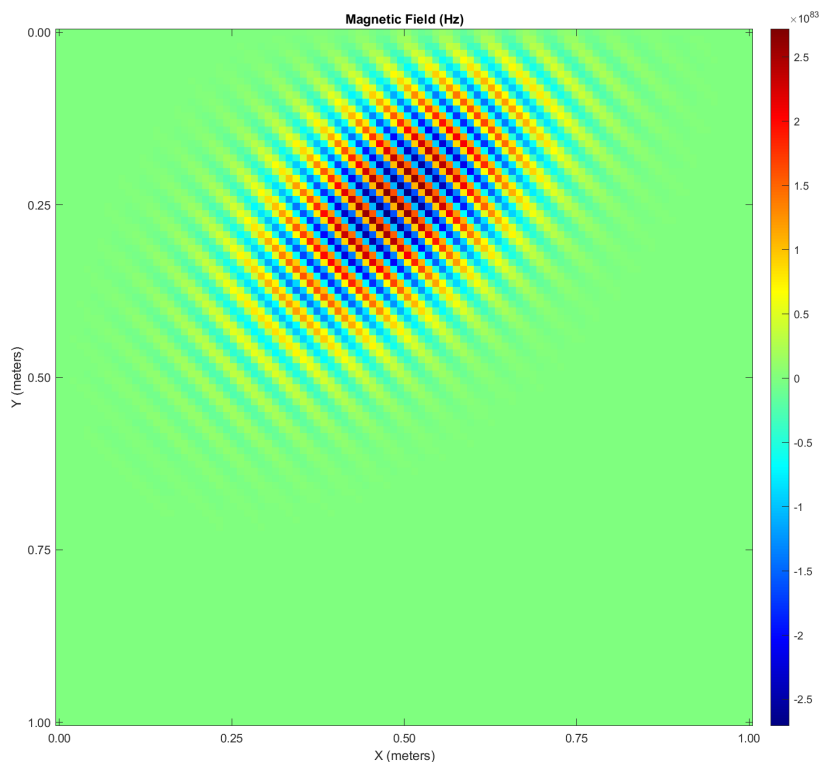
```

112 y_tick_labels = sprintfc('%f', y_label_vals*dy);
113 xticks(x_ticks);
114 yticks(y_ticks);
115 xticklabels(x_tick_labels);
116 yticklabels(y_tick_labels);
117 xlabel('X (meters)');
118 ylabel('Y (meters)');
119 axis equal;
120 colormap(jet);
121 colorbar;

```

5.2 Result of the Simulation

Having executed the code, we get the following results



The simulation result

Figure 5.1: The simulation result

This figure is generated after the completion of the time-stepping loop (once the simulation is finished). It shows a 2D representation of the final magnetic field H_z in the simulation domain where the x-axis corresponds to the spatial points in the x-direction (number of points is the variable `num_points_x`). The y-axis corresponds to the spatial points in the y-direction (the number of points is the variable `num_points_y`).

The reader may notice the unreasonable values that the component H_z attends. In actuality, it is a result of the Gaussian pulse generation and accumulation over time. Depending on the specific parameters of the Gaussian pulse (`pulse_amplitude`, `pulse_width`, and `pulse_decay_factor`), it's possible for the field values to grow or decay over time.

For example, if the `pulse_amplitude` is large, and the `pulse_decay_factor` is close to 1.0, the magnitude of the pulse

may accumulate over time, leading to larger values in the H_z field during the simulation.

APPENDIX

Bibliography

- [1] D. M. Pozar, *Microwave engineering; 3rd ed.* Hoboken, NJ: Wiley, 2005.
- [2] K. W. Kark, *Antennen und Strahlungsfelder; 8th ed.* Springer Vieweg Wiesbaden, 2020.
- [3] B. Salamito, M.-N. Sanz, F. Vandembrouck, and M. Tuloup, *Physique - Tout-en-un - MP, MP**. 5 rue Laromiguière, 75005 Paris: Dunod, 2014.
- [4] B. Salamito, D. Jurine, S. Cardini, and M.-N. Sanz, *Physique - Tout-en-un - MPSI, PTSI*. 5 rue Laromiguière, 75005 Paris: Dunod, 2013.
- [5] R. Severns, *Antennas with Gain and Bandwidth for 80 and 160 Meters*. PO Box 589, Cottage Grove, OR 97424: ARRL National Contest Journal, 2000.
- [6] S.-Y. Chen, "Broadband slot-type birc array fed by a microstrip-to-slotline t-junction," *IEEE Antennas and Wireless Propagation Letters*, vol. 8, pp. 116–119, 2009.
- [7] Z. Ahmed, M. H. Hoang, P. McEvoy, and M. J. Ammann, "Millimetre-wave planar birc array antenna," in *2020 International Workshop on Antenna Technology (iWAT)*, pp. 1–3, 2020.
- [8] K. I. Kellermann, E. N. Bouton, and S. S. Brandt, *Open Skies: The National Radio Astronomy Observatory and Its Impact on US Radio Astronomy*. Cham: Springer International Publishing, 2020.
- [9] M. Bartsch, M. Dehler, M. Dohlus, F. Ebeling, P. Hahne, R. Klatt, F. Krawczyk, M. Marx, Z. Min, T. Pröpper, D. Schmitt, P. Schütt, B. Steffen, B. Wagner, T. Weiland, S. G. Wipf, and H. Wolter, "Solution of maxwell's equations," *Computer Physics Communications*, vol. 73, no. 1, pp. 22–39, 1992.
- [10] N.D, *CST MICROWAVE STUDIO Workflow & Solver Overview*. CST-Computer Simulation Technology AG, 2016.